problems of neutron detector absorption, source perturbation, and mode content control (or use of an integrating technique).[3] The first of these has been properly dealt with in the present experiment. The second may produce some slight systematic error; its magnitude is difficult to evaluate. The third represents the principal source of possible systematic error. The studies of Mead, England, Collie, and Weeks,[2] using a very large moderator and a comparatively low-energy neutron source showed definite evidence of a mixture of modes present after rather long delays, yet the composite decay curve was very nearly exponential. The "mode suppression factors" calculated (for a fission source) by Holzer and Crouch[3] show that in the present case there is some appreciable suppression of higher modes, though somewhat smaller moderators would be necessary for complete suppression. Moreover, the agreement of measured mean lifetime values for the two sizes of moderators used, and the similarity in shape of the delay distributions at early delay times, suggest that the admixture of higher modes is probably small. Nevertheless the present measurement must be considered to have some possible systematic error from this cause.

A new measurement is in progress at this laboratory in which source perturbation is greatly reduced and mode content controlled by a mode synthesis procedure.

ACKNOWLEDGMENT

The authors wish to express their thanks to Professor L. L. Foldy for helpful discussions and important suggestions in connection with the "asymptotic approximation" calculations.

PHYSICAL REVIEW VOLUME 114, NUMBER 6 JUNE 15, 1959

Elastic Scattering of 3.7-Mev Neutrons from S, Fe, Co, Ni, Cu, and Zn†

M. K. MACHWE,* D. W. KENT, JR., AND S. C. SNOWDON
Bartol Research Foundation of the Franklin Institute, Swarthmore, Pennsylvania

(Received December 1, 1958)

The differential cross section for the elastic scattering of 3.7-Mev neutrons from sulfur, iron, cobalt, nickel, copper, and zinc has been measured in a ring geometry using a modified Bonner-type scintillation detector. The measurements were taken over an angular range between 10° and 160°. Angular resolution effects have been removed by a suitable iterative procedure. Multiple-scattering effects have been removed by an approximate analytical treatment.

I. INTRODUCTION

THE present series of measurements of the differential cross sections for 3.7-Mev neutrons elastically scattered from sulfur, iron, cobalt, nickel, copper, and zinc are a continuation of similar measurements reported by us.[1,2]

In a recent set of measurements[2] we used a Bonner-type detector consisting of a network of spheres. A series of tests showed, however, that the use of more than one small scintillant fails to achieve the expected increase in over-all detector efficiency for counting elastically scattered neutrons. This deficiency is attributed to the varying efficiency with which light is collected from the individual scintillators. In fact, a detector made with only one cylinder of plastic scintillant 0.1 inch in diameter and 0.1 inch high produced nearly the same proton recoil counting rate in the acceptable part of the spectrum as did the detector that made use of eight spheres of plastic scintillant 0.1 inch in diameter.

Since there appears to be no large gain in counting rate accompanying the use of a multiple plastic ball detector over that of the single plastic cylinder, and since the angular resolution corrections are simplified with the detector of smaller physical size, we have carried out the present measurements with a single plastic cylinder detector.

II. EXPERIMENTAL PROCEDURE

Figure 1 shows the scattering geometry. Neutrons of about 3.7 Mev are produced by allowing a 40-microampere, 1.0-Mev deuteron beam to impinge on a deuterium gas cell filled to one atmosphere pressure. The mean energy of neutrons in the forward direction is 3.66 Mev with a spread in energy of about 400 kev. The forward-direction neutron detector consists of a 0.1-inch diameter, 0.1-inch high plastic scintillator placed directly on the face of a DuMont type K-1382 photomultiplier. For purposes of normalizing each data run, a scintillation detector, similar to the forward-

† Assisted by the U. S. Atomic Energy Commission.
* Research fellow, Bartol: Now at Université de Montreal. Contents of this paper submitted to the Delhi University, Delhi, India, in partial fulfillment of the requirements for the degree of Doctor of Philosophy.
[1] W. D. Whitehead and S. C. Snowdon, Phys. Rev. **92**, 114 (1953); S. C. Snowdon and W. D. Whitehead, Phys. Rev. **94**, 1267 (1954).
[2] H. S. Hans and S. C. Snowdon, Phys. Rev. **108**, 1028 (1957).

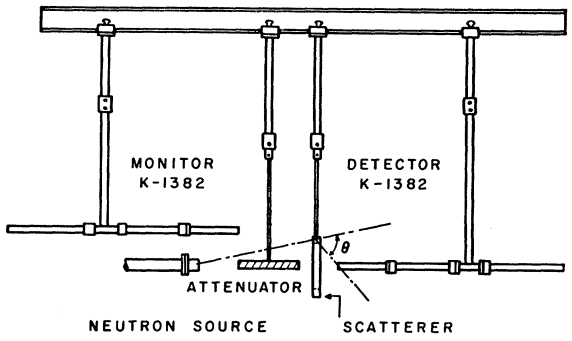

FIG. 1. Ring geometry for scatterer.

direction detector, detects neutrons emitted by the source at an angle of about 40°.

Scattering angles between 10° and 160° are obtained by using a series of three ring scatterers: a 7-inch mean diameter ring with a $\frac{3}{4}$-inch square cross section, a 5-inch mean diameter ring with a $\frac{3}{4}$-inch square cross section, and a 3-inch mean diameter ring with a $\frac{3}{4}$-inch square cross section. A ring is mounted so that its axis coincides with the deuteron beam axis as shown in Fig. 1. Movement of a ring along this axis provides the desired variation of scattering angle.

Analysis of the pulses derived from recoil protons and electrons was accomplished using a 20-channel analyzer. A precision pulse applied at the last dynode of the photomultiplier was used continuously to monitor changes in all electronics except the photomultiplier. Frequent checks were made of the stability of the high voltage applied to the photomultiplier. In addition, frequent checks were made of the gain of the amplifier plus pre-amplifier system.

A similar electronic detection and stability monitoring system was used for the neutron monitor photomultiplier. Since, in this case, it was not necessary to have detailed pulse-height analysis, a single-channel analyzer was used to accept the upper part of the recoil proton spectrum and reject the test pulse.

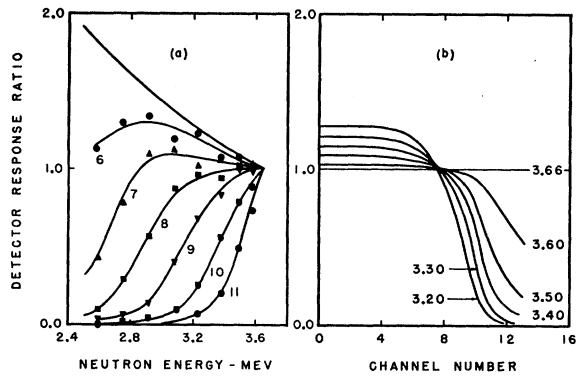

FIG. 2. Detector response: (a) response of proton recoil scintillation detector for several channels of the multichannel pulse-height analyzer as a function of neutron energy. The response in all channels for neutrons of 3.66 Mev, the forward direction energy, is taken as unity. The unlabeled curve, normalized to unity at 3.66 Mev, is a plot of the n-p cross section divided by the neutron energy. The figure (b) contains the same information as (a) except that it is plotted in a form more suitable for determining the scattering ratio spectra.

A typical run of data for the determination of the differential elastic scattering cross section at a fixed angle is as follows. The recoil proton pulse-height spectrum of the direct neutron beam is observed for a standard number of counts in the neutron monitor scaler; a background spectrum is observed for the same number of monitor counts by interposing the attenuator between the source and the detector; the scattering ring then is placed in location and a pulse-height spectrum recorded for the same number of monitor counts. From these three spectra a "ratio spectrum" is computed by taking, for each channel, the ratio of scattered neutron counts corrected for background to the direct neutron counts corrected for background. A typical ratio spectrum is shown in Fig. 3.

The structure of a typical ratio spectrum may be interpreted by considering the following features: (1), the change in energy of the scattered neutron with respect to the energy of the direct neutron beam; (2), the presence of inelastically scattered neutrons and associated γ-rays produced in the scattering rings. In order to investigate the effects of energy changes in the ratio spectrum, one makes use of the connection between the angle of emission and the energy of the neutron emitted in the d-D reaction.[3] Proton recoil pulse-height spectra are obtained at several angles of emission. Each pulse-height spectrum is normalized to unit neutron flux by dividing by the expected neutron yield for that angle.[4] The ratio of this normalized spectrum to a similar spectrum for zero-angle gives directly the ratio-spectrum for 100% scattering of neutrons having an energy corresponding to the selected angle. Figure 2 shows the measured detector response for several useful channels. The limiting curve in Fig. 2(a) is a curve of $\sigma(E_N)/E_N$ normalized to unity at $E_N=3.66$ Mev. The validity of assuming this curve to be the zero channel response was strengthened by demonstrating that the yield of the proton recoil pulses taken at the inflection end point varies as $\sigma(E_N)/E_N$ times the neutron yield from the d-D reaction. Figure 2(b) is a plot of Fig. 2(a) *versus* channel for several neutron energies useful in reducing the data.

Figure 3 reveals the method by which the neutron scattering ratio is found in a typical case. For a given scattering angle the energy of the scattered neutron is computed. The ratio spectrum for 100% scattering at this energy is found from Fig. 2(b). This ratio spectrum is multiplied by a number which is adjusted until a good fit is obtained with the measured ratio spectrum in the upper channels where only elastic scattering is expected to be present. Curve (a) in Fig. 3 shows the

[3] J. L. Fowler and J. E. Brolley, Jr., Revs. Modern Phys. **28**, 103 (1956).

[4] Fuller, Dance, and Ralph, Phys. Rev. **108**, 91 (1957).

result of this fitting process. The rise in the measured ratio spectrum as shown in curve (b) of Fig. 3 is due to the presence of inelastically scattered neutrons and γ-rays associated with those inelastic events. The number found in the curve-fitting process is normalized to unit angular sensitivity of the neutron detector by dividing by the measured angular sensitivity given in Fig. 4. The result is then the neutron scattering ratio S.

The neutron scattering ratio may be written as

$$S=S_1+S_2+S_3+\cdots, \quad (1)$$

where S_1, S_2, etc., are the contributions to the scattering ratio from neutrons singly scattered, doubly scattered, etc. The principal contribution is from single scattering S_1, where

$$S_1=\int_V \frac{I(\theta_1)}{I(0)}\left(\frac{R_0}{R_1R_2}\right)^2\sigma(\theta)ne^{-\sigma_{tot}n(r_1+r_2)}dV. \quad (2)$$

The number of scattering nuclei per unit volume is n, and $\sigma(\theta)$ is the differential cross section for scattering into the laboratory angle θ. All geometrical quantities are shown in Fig. 5. $I(\theta_1)$ is the yield of the d-D reaction at an angle θ_1. Analogous expressions for double, triple, etc., scatterings contain double, triple, etc., volume integrals.

In order to obtain the desired single-scattering ratio S_1 from the net scattering ratio S, multiple-scattering contributions amounting to about 15% must be removed or accounted for. Our previous work[2] made use of a Monte Carlo technique in which one follows many case histories of a neutron traversing the scattering ring. We have subsequently shown that, in the case of our previous work, a very close approximation to the Monte Carlo result may be obtained by the following simple analytical method. Assume that it is quite probable that each of the multiple scatterings that subsequently enter the neutron detector has a large probability of occurring in the following way. All neutron scatterings except one are zero-angle scatterings, the remaining one being scattered through an angle appropriate to send it in the direction of the neutron detector. As a partial justification for this assumption, we note that neutron scattering at this energy is strongly peaked in the forward direction. The result of this assumption is to permit each higher order scattering ratio to be evaluated in terms of a single volume integral. Thus Eq. (1) becomes

$$S=\int_V \frac{I(\theta_1)}{I(0)}\left(\frac{R_0}{R_1R_2}\right)^2\sigma(\theta)n\left\{1+\sigma_{el}n(r_1+r_2)+\frac{1}{2!}\sigma_{el}^2n^2(r_1+r_2)^2+\cdots\right\}e^{-\sigma_{tot}n(r_1+r_2)}dV. \quad (3)$$

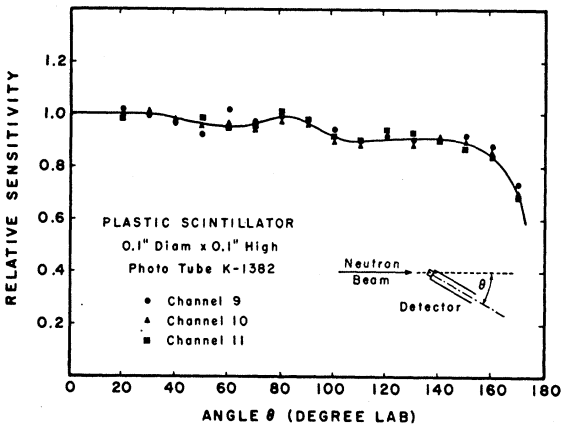

FIG. 4. Response of scintillation detector to neutrons entering at several angles with respect to the axis of the detector. The response is normalized to unity for neutrons entering along the axis.

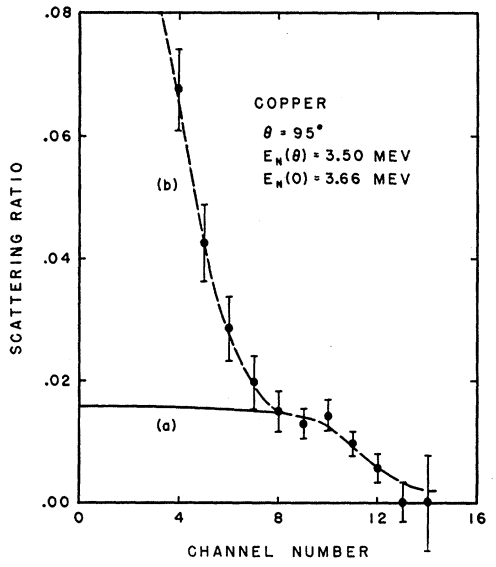

FIG. 3. Typical scattering ratio curve. Part (a) is a multiple of the detector response ratio in Fig. 2(b) for a neutron energy of 3.50 Mev. Part (b) is the measured scattering ratio. The deviation between parts (a) and (b) is due to the presence of inelastically scattered neutrons and their associated γ rays.

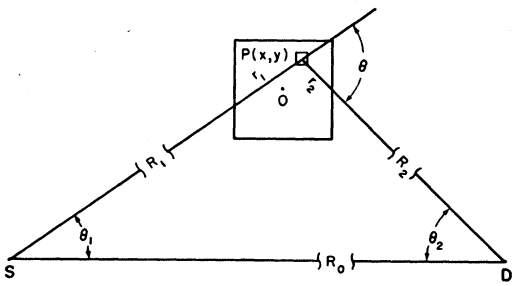

FIG. 5. Details of scattering geometry. The point $P(x,y)$ is depicted within the cross section of the scattering ring. S and D represent the location of the source and detector, each of which may be considered as geometrical points when compared with the extent of the ring cross section.

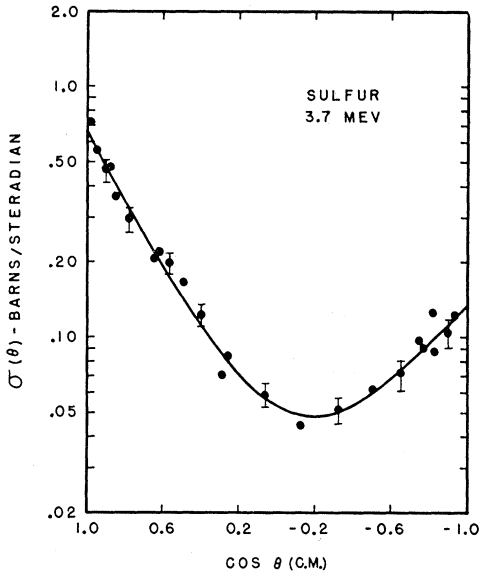

FIG. 6. Measured differential cross section for the elastic scattering of 3.7-Mev neutrons by sulfur.

Since the sum in the bracket is $e^{\sigma_{el} n(r_1+r_2)}$ we see that, using the above approximation, Eq. (2) for S_1 now holds for the net scattering ratio S if σ_{tot} is replaced by σ_{nonel}. Thus

$$S=\int_V \frac{I(\theta_1)}{I(0)}\left(\frac{R_0}{R_1R_2}\right)^2\sigma(\theta)ne^{-\sigma_{nonel}n(r_1+r_2)}dV. \quad (4)$$

Physically, this means that the attenuation of the neutron beam into and out of the ring occurs only by true absorption and not by elastic scattering. This

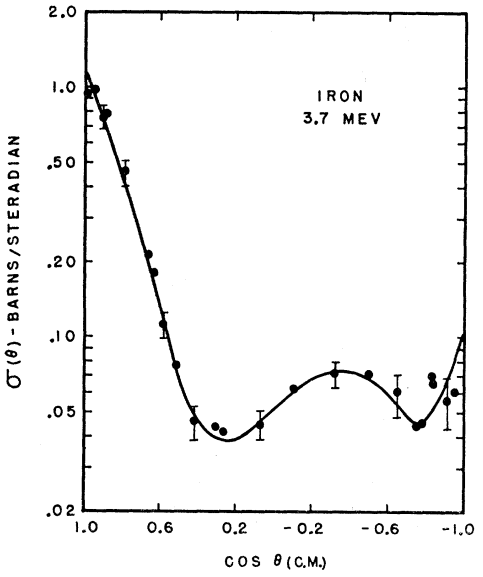

FIG. 7. Measured differential cross section for the elastic scattering of 3.7-Mev neutrons by iron.

cannot of course be completely true. However, the scattering ratio calculated using Eq. (4) agrees with the more accurate Monte Carlo method within a statistical accuracy of 6% in the particular case of zirconium.[2] Since the explanation for the approximation given by Eq. (4) is plausible, we have assumed that the use of Eq. (4) reduces the multiple-scattering contribution to not more than 5%.

In order to make use of Eq. (4) to obtain the differential elastic scattering cross section $\sigma(\theta)$ from the measured scattering ratio S, the following method is employed. Expand all quantities in the integrand except those in the exponential about their mean values, retaining terms up to the second order. For convenience, the center of the cross section of the ring is used in defining the mean values of the quantities

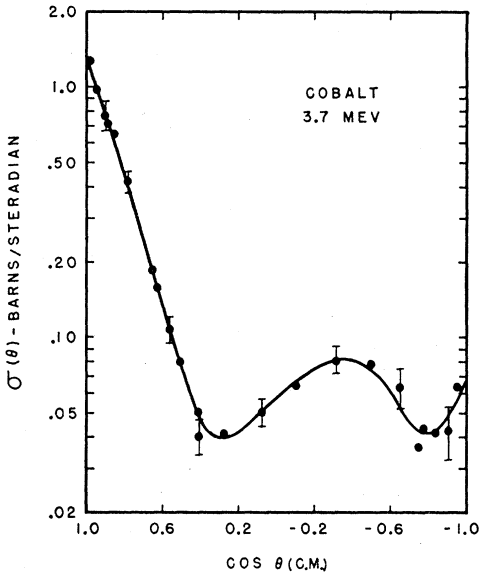

FIG. 8. Measured differential cross section for the elastic scattering of 3.7-Mev neutrons by cobalt.

involved. Evaluate the volume integrals numerically for each location of the ring assuming a trial value for the nonelastic cross section σ_{nonel}. Since the expansion of $\sigma(\theta)$ will involve the first and second derivatives of $\sigma(\theta)$, these are approximated by first finding the $\sigma(\theta)$ that obtains if all quantities under the integral except the exponential are treated as constants. The first and second derivatives of this $\sigma(\theta)$ then are found by using an 11-point Lagrange differentiation formula.[5] Carrying out these operations yields a value for the differential cross section which is quite accurate except for the assumed σ_{nonel}. However, since the total cross section is measured for each element in the same geometry and since the nonelastic cross section σ_{nonel} is equal to $\sigma_{tot}-\int\sigma(\theta)d\Omega$, it is possible to carry out a calculation which yields $\sigma(\theta)$ that is consistent with the above

[5] W. G. Bickley, Math. Gazette 25, 19 (1941).

relation. This calculation, of course, also gives the correct σ_{nonel}.

III. EXPERIMENTAL RESULTS

Figures 6–11 show the experimental results of our measurement of the differential cross sections for the elastic scattering of 3.7-Mev neutrons from sulfur, iron, cobalt, nickel, copper, and zinc. All quantities plotted are in the center-of-mass coordinates. The solid curves drawn through the points are visual estimates of the best curves to be obtained from the data points. The error bars represent the resultant standard deviation of the measurements compounded from estimates to be given in the section on errors.

Previous measurements of the differential cross section for the elastic scattering of 3.7-Mev neutrons

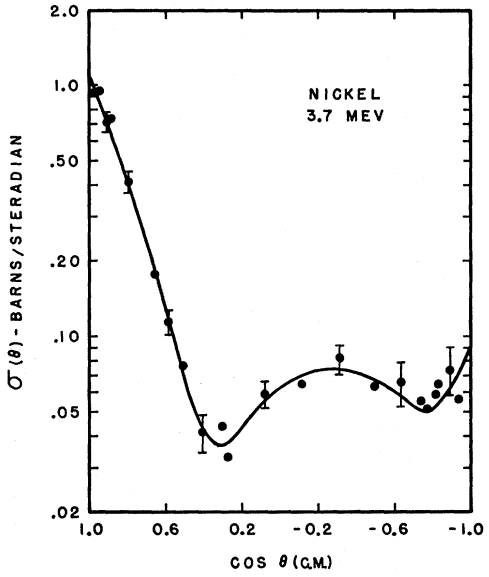

FIG. 9. Measured differential cross section for the elastic scattering of 3.7-Mev neutrons by nickel.

have been made by Morgan[6] for the elements sulfur and copper. These measurements are some 30 to 50% higher than our measurements. A possible explanation may be that the measurements reported by Morgan[6] include some inelastically scattered neutrons since his detector, a Hornyak-type scintillator, is known not to discriminate against inelastically scattered neutrons as effectively as the Bonner-type detector.

A comparison of our differential cross sections for iron and zinc at 3.7-Mev with those of Beyster, Walt, and Salmi[7] at 4.1 Mev shows fair agreement. The general features agree over all angles common to both

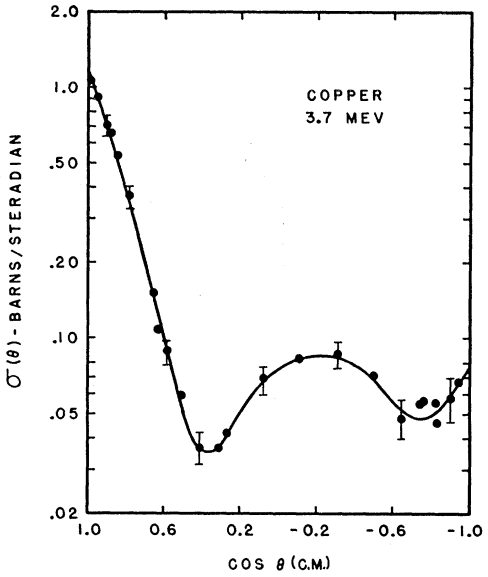

FIG. 10. Measured differential cross section for the elastic scattering of 3.7-Mev neutrons by copper.

sets of data; the extreme forward scattering and extreme backward scattering, however, differ by as much as 40%.

Table I presents the results of a Legendre polynomial analysis of the solid curves in Figs. 6–11 using a method of analysis developed especially for this purpose.[8] The table presents the coefficients B_L in the expression

$$\sigma(\theta)=\frac{1}{4\pi}\sum(2L+1)B_L P_L(\cos\theta),$$

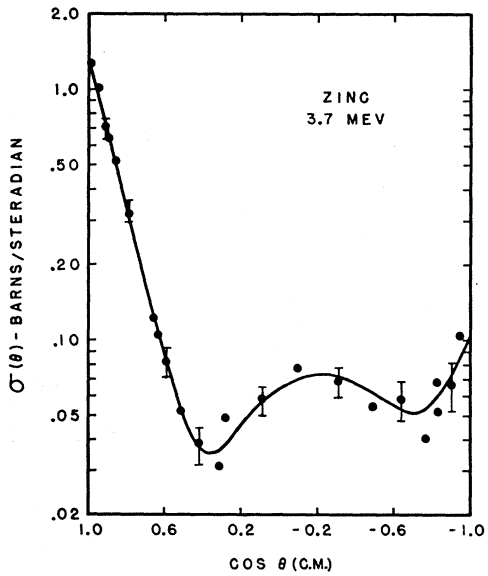

FIG. 11. Measured differential cross section for the elastic scattering of 3.7-Mev neutrons by zinc.

[6] I. L. Morgan, reported in Brookhaven National Laboratory Report BNL-400, edited by D. J. Hughes and R. S. Carter (unpublished).

[7] Beyster, Walt, and Salmi, Phys. Rev. **104**, 1319 (1956); M. Walt and J. R. Beyster, Phys. Rev. **98**, 677 (1955).

[8] Snowdon, Eisenbud, and Marshall, J. Appl. Phys. **29**, 950 (1958).

TABLE I. Legendre coefficient B_L in $\sigma(x)=(1/4\pi)\Sigma(2L+1)B_LP_L(x)$. Units of $\sigma(x)$ are barns per steradian. Total and integrated cross sections are in barns.

L	Sulfur	Iron	Nickel	Cobalt	Copper	Zinc
0	1.797±0.075	1.898±0.100	1.822±0.100	1.973±0.100	1.810±0.100	1.747±0.100
1	0.679±0.037	0.989±0.034	0.917±0.034	1.051±0.034	0.863±0.034	0.871±0.034
2	0.535±0.060	0.769±0.078	0.716±0.078	0.804±0.078	0.684±0.078	0.736±0.078
3	0.156±0.025	0.479±0.027	0.461±0.027	0.533±0.027	0.476±0.027	0.515±0.027
4	0.068±0.035	0.232±0.045	0.233±0.045	0.267±0.045	0.274±0.045	0.321±0.045
5	0.017±0.013	0.039±0.013	0.050±0.013	0.061±0.013	0.058±0.013	0.119±0.013
6	0.007±0.010	0.016±0.010	0.017±0.010	0.029±0.010	0.016±0.010	0.054±0.010
$\sigma_{\text{tot el}}$	1.80 ±0.08	1.90 ±0.10	1.82 ±0.10	1.97 ±0.10	1.81 ±0.10	1.75 ±0.10
σ_{tot}	2.58 ±0.09	3.41 ±0.14	3.33 ±0.15	3.59 ±0.15	3.38 ±0.15	3.59 ±0.17
σ_{nonel}	0.78 ±0.12	1.51 ±0.17	1.51 ±0.18	1.62 ±0.18	1.57 ±0.18	1.84 ±0.20

where all quantities refer to the center-of-mass coordinates.

IV. ERRORS

The uncertainty in the final differential cross section is estimated from six sources of error in addition to the counting statistics.

(1) The uncertainty in the multiple-scattering correction inherent in the approximate analytical treatment. This is estimated to be not more than ±5% and is largest near the minima in the curves.

(2) The uncertainty in the solution of Eq. (4) for $\sigma(\theta)$ by a finite rather than an infinite iteration. It is estimated that this approximation leaves a residual uncertainty in $\sigma(\theta)$ of about ±5% at the minima of the curves.

(3) Geometrical uncertainties. These amount to ±1%.

(4) Variations in background between successive ring-in, ring-out readings including scattering-in of background neutrons, attenuation of background neutrons, and variations difficult to detect. Auxiliary tests indicate that the uncertainty for this measurement is not greater than about ±3%.

(5) Target pressure and foil thickness variations. These variations change the effective energy and flux distribution of the emitted neutrons and represent an uncertainty of about ±3%.

(6) The polarization of neutrons from the $H^2(d,n)He^3$ reaction.[9] Under our experimental conditions the polarization is not greater than 7%. Assuming that the scatterings are 100% effective in distinguishing spin-up from spin-down neutrons, the polarization would then lead to a 7% error. However, the measured polarization asymmetry for copper is not larger than 40%[10]; hence, we conclude that the uncertainty caused by the polarized neutron source is probably less than 3%.

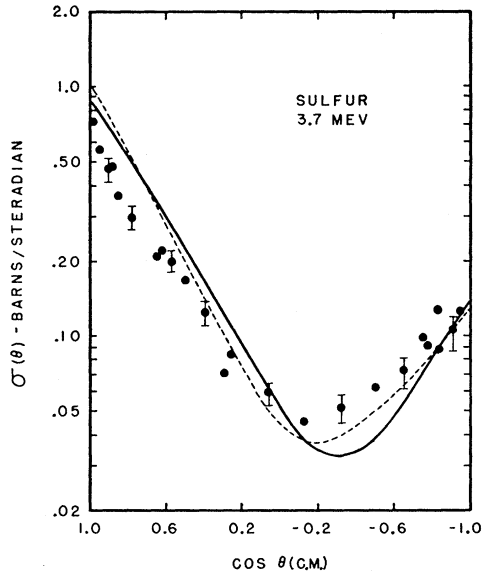

FIG. 12. Comparison of measured differential cross section with optical model calculations for sulfur. Solid curve is case (1) and dotted curve is case (2).

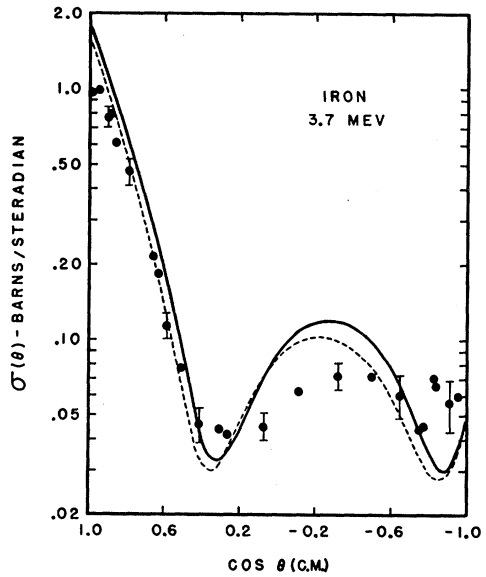

FIG. 13. Comparison of measured differential cross section with optical model calculations for iron. Solid curve is case (1) and dotted curve is case (2).

[9] R. E. Segel and S. S. Hanna, Phys. Rev. **106**, 536 (1957). These authors present a summary of recent measurements of the polarization of the $H^2(d,n)He^3$ reaction.

[10] McCormac, Steuer, Bond, and Hereford, Phys. Rev. **108**, 116 (1957).

The statistical uncertainty in the measurements was determined by the standard deviation of the neutron scattering ratio obtained in the curve-fitting process. This contribution varies from about $\pm 5\%$ for small angles to about $\pm 20\%$ for the backward angles. Since a liberal estimate is given for each source of error it was felt that the root-mean-square error would be a realistic estimate of the net uncertainty.

Some checks on more subtle flux variations within a run, and on the presence of time-dependent systematic errors were made by examining the internal consistency of the data. In particular, at least three independent measurements of the entire angular distribution were made for each element. The deviations of each run from the mean of three runs were in close agreement with that expected from the statistical errors in each individual run, indicating satisfactory reproducibility in the data. Another check was made by measuring the neutron scattering ratio at three angles with rings of different diameter and hence different geometry. The measurements showed no systematic variation in S as a function of ring diameter.

In addition, for completeness, the table gives the total elastic cross section given by the value of B_0, the total cross section measured in this experiment, and the nonelastic cross section.

V. DISCUSSION

Bjorklund and Fernbach[11] have carried out optical model calculations at 4.1 Mev in which the parameters determining the shape of the central potentials were determined mainly by using the 14-Mev data. The strengths of the central potentials and of the spin-orbit terms then were varied to produce a best fit to the 4.1-Mev data of Beyster, Walt, and Salmi.[7] A comparison of our data for iron and zinc with the calculations of Bjorklund and Fernbach indicates a discrepancy that is of the order of the difference between the two sets of data. Since there are no calculations at 3.7 Mev comparable in detail with those of Bjorklund and Fernbach at 4.1 Mev, our data are compared in Figs. 12–17 with the computations of Reilly and

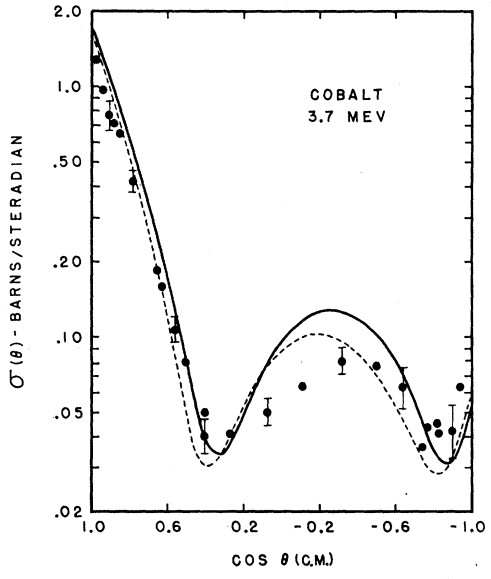

FIG. 14. Comparison of measured differential cross section with optical model calculations for cobalt. Solid curve is case (1) and dotted curve is case (2).

[11] F. Bjorklund and S. Fernbach, Phys. Rev. **109**, 1295 (1958).

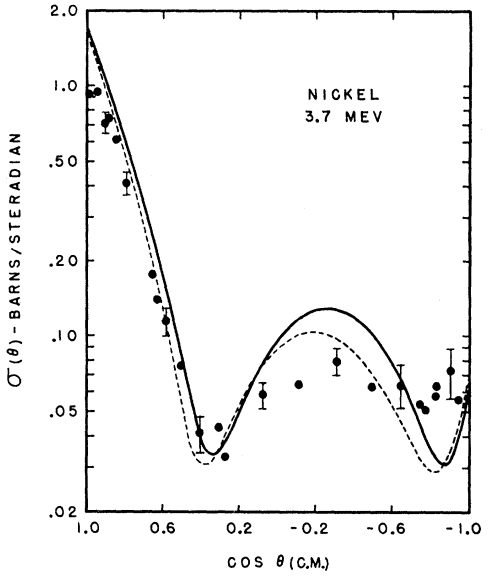

FIG. 15. Comparison of measured differential cross section with optical model calculations for nickel. Solid curve is case (1) and dotted curve is case (2).

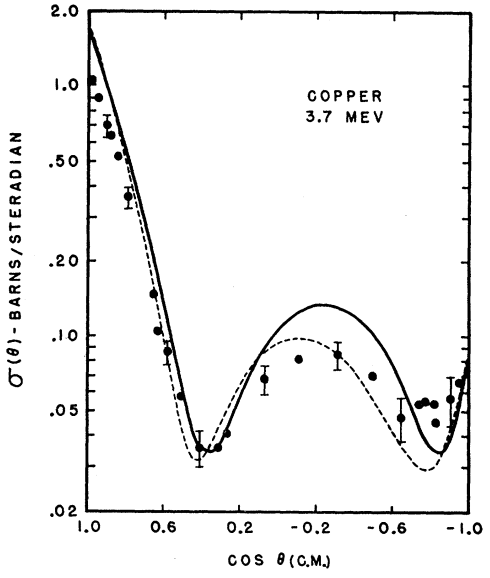

FIG. 16. Comparison of measured differential cross section with optical model calculations for copper. Solid curve is case (1) and dotted curve is case (2).

TABLE II. Integrated cross sections from optical model.

Element	Case (1) r_0 (fermi)	ξ	$\sigma_{\text{shape el}}$ (barns)	$\sigma_{\text{compound el}}$ (barns)	σ_{tot} (barns)	σ_{nonel} (barns)	Case (2) r_0 (fermi)	ξ	$\sigma_{\text{shape el}}$ (barns)	$\sigma_{\text{compound el}}$ (barns)	σ_{tot} (barns)	σ_{nonel} (barns)
S	1.20	0.100	1.90	0.38	2.80	0.52	1.25	0.120	1.87	0.45	3.04	0.72
Fe	1.20	0.100	2.31	0.38	3.58	0.89	1.25	0.140	2.01	0.28	3.49	1.20
Co and Ni	1.20	0.100	2.24	0.38	3.50	0.88	1.25	0.145	1.95	0.28	3.53	1.30
Cu	1.20	0.100	2.12	0.38	3.44	0.94	1.25	0.149	1.90	0.28	3.65	1.47
Zn	1.20	0.100	2.11	0.38	3.44	0.95	1.25	0.150	1.89	0.28	3.68	1.51

Francis[12] at 3.7 Mev. These workers employ a diffuse surface potential well and account for compound elastic scattering but omit the spin-orbit interaction.

The optical potential used by Reilly and Francis was of the Woods-Saxon type,[13]

$$V(r)=-\frac{V_0(1+i\xi)}{1+e^{(r-R)/a}}.$$

Two sets of parameters were chosen: case (1) used

$$V_0=42.0 \text{ Mev}, \quad \xi=0.1,$$
$$R=0.8+1.2A^{\frac{1}{3}} \text{ fermi}, \quad a=0.35 \text{ fermi};$$

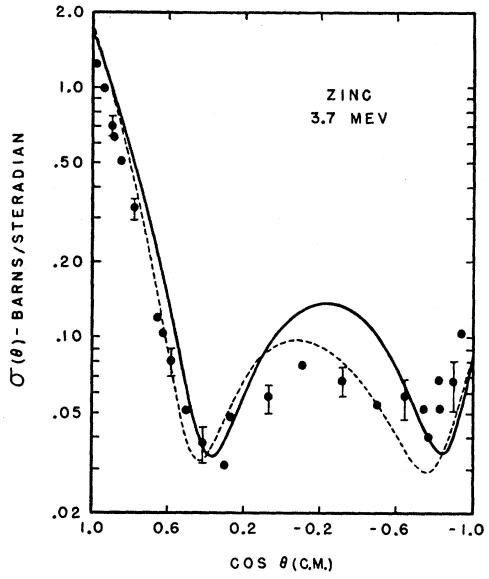

FIG. 17. Comparison of measured differential cross section and optical model calculations for zinc. Solid curve is case (1) and dotted curve is case (2).

and case (2) used

$$V_0=42.0 \text{ fermi}, \quad \xi \text{ given in Table II},$$
$$R=0.8+1.25A^{\frac{1}{3}} \text{ fermi}, \quad a=0.35 \text{ fermi}.$$

The parameters in case (1) gave a very good fit to our total cross section measurements, but did not give a very good fit to the nonelastic cross sections computed by subtracting our integrated elastic cross sections from our corresponding total cross sections. On the other hand, if the parameters in case (2) are used, the nonelastic cross sections may be fitted very well but at the expense of the good fit to the total cross sections obtained in case (1). No further adjustment of the parameters in the optical model was carried out. Table II summarizes the results of the present calculations. In each case an estimate had to be made of the contribution to the elastic scattering due to compound-elastic scattering. The estimated compound-elastic contribution is roughly consistent with that obtainable from the theory of Hauser and Feshbach[14] and is assumed to be isotropically distributed.

ACKNOWLEDGMENTS

The authors wish to express their appreciation to W. F. G. Swann, Director of the Bartol Research Foundation, for his continued interest in elastic neutron scattering. Our thanks are also due to H. S. Hans, now at Muslim University, Aligarh, who participated in the early phases of this work. Finally, the authors appreciate the efforts of E. D. Reilly, Jr., and N. C. Francis in making available the optical model calculations with which our data were compared and to P. F. Zweifel, who expedited these calculations at the Knolls Atomic Power Laboratory.

[12] E. D. Reilly and N. C. Francis, Knolls Atomic Power Laboratory (private communication).

[13] R. D. Woods and D. S. Saxon, Phys. Rev. **95**, 577 (1954).

[14] W. Hauser and H. Feshbach, Phys. Rev. **87**, 366 (1952).